

Interface modification of ITO thin films: organic photovoltaic cells

Neal R. Armstrong^{a,*}, Chet Carter^a, Carrie Donley^a, Adam Simmonds^a, Paul Lee^a,
Michael Brumbach^a, Bernard Kippelen^b, Benoit Domercq^b, Seunghyup Yoo^b

^aDepartment of Chemistry, University of Arizona, Tucson, AZ 85721, USA

^bOptical Sciences Center, University of Arizona, Tucson, AZ 85721, USA

Abstract

In this paper we review our recent studies of the surface characterization of commercially available indium-tin-oxide (ITO) thin films, using photoelectron spectroscopies (XPS and UPS) and electrochemistry of chemisorbed probe molecules such as ferrocene dicarboxylic acid (Fc(COOH)₂). The modification of these ITO films through chemisorption of carboxylic acid-substituted small molecules, such as Fc(COOH)₂, 3-thiophene acetic acid (3-TAA), and the subsequent modification of these interfaces with electrochemically grown conducting polymer (CP) films is also introduced. We report preliminary results of our studies changes in performance of vacuum deposited organic photovoltaic (PV) cells as a result of these ITO substrate modification steps. The surfaces of as-received ITO films, and those cleaned by various solution and plasma-etching processes, are unavoidably hydrolyzed to In(OH)₃-like and InOOH-like surface species, which leaves the ITO surface with at most 40–50% of the electronically active sites available for electron transfer reactions. Modification of the ITO surface with electroactive small molecules such as Fc(COOH)₂ and 3-TAA provides for better wettability of organic layers to the polar ITO surface and enhanced electrical contact (lower series resistance, R_s) between the ITO anode, spin-cast or electrodeposited PEDOT:PSS layers and copper phthalocyanine (CuPc) layers in multilayer (CuPc/C₆₀/BCP) excitonic PV cells. Improvements in PV J/V (current/voltage) responses are noted mainly through increases in short-circuit photocurrent and lowered series resistances (R_s) when electroactive small molecules are chemisorbed to the ITO surface, prior to spin-casting of conducting polymer, PEDOT:PSS, layers.

© 2003 Elsevier B.V. All rights reserved.

Keywords: Photovoltaic; Indium-tin-oxide (ITO); Copper phthalocyanine

1. Introduction

The continuing development of organic light emitting diode (OLED) technologies and the interest in significantly improving the efficiency of organic photovoltaic (PV) cells has intensified the need to understand and control the transparent conductive oxide (TCO) substrates (e.g. indium-tin oxide, ITO, and antimony-doped or fluorine-doped tin-oxide, d-SnO₂) upon which these organic thin film technologies are generally deposited [1–25]. Several studies of both small molecule and polymer-based OLED technologies have shown that the surfaces of these polar hydrophilic oxides are often chemically incompatible with non-polar organic thin films, leading to delamination of the organic layers and high series resistances in either OLED or PV cells. High and reproducible work functions are also difficult to

obtain for these TCOs, making ohmic contacts difficult to achieve, and further increasing the series resistances in these devices. The chemical instability of the near-surface region of ITO substrates may, in addition, necessitate chemical modification of these oxide films. Strategies have been developed to increase the wettability of the ITO surface by these non-polar organic thin films, to tune the effective work function of this material through chemisorption or covalent attachment of polar organic functional groups, and to balance the rate of hole injection at the ITO anode with electron injection at the cathode, through the introduction of ‘blocking’ layers at the ITO surface, which also increase anode stability [1–4,8–18]. Several recent accounts have discussed the role of surface cleaning/pretreatments on ITO surface energies, and on the correlation of these surface energies with OLED performance, and additional studies have shown that doping the hole-transport layers at the ITO interface improves both stability and OLED

*Corresponding author.

E-mail address: nra@u.arizona.edu (N.R. Armstrong).

efficiency [2–4,8–15]. It is clear that many of the issues faced in OLED optimization will also be of importance for improving efficiencies of organic thin film PV cells, where ITO, doped-SnO₂, and related TCOs are anticipated to be the anode materials of choice, either on glass substrates, or more preferably on flexible, light plastic substrates.

ITO thin film electrodes have also recently played a key role in transmission and integrated optical spectro-electrochemical characterization of redox reactions of adsorbed proteins and molecular assemblies, and as electrochemical bio-sensor platforms [26,27]. Many of the instabilities and compatibility issues arising with OLED and PV technologies also arise in the optimization of these technologies, where rapid electron transfer involving adsorbed monolayers of organic molecule, is desired.

In this paper we review some of our recent studies of surface composition of commercial sputter-deposited ITO thin films, using monochromatic X-ray photoelectron spectroscopy and UV-photoelectron spectroscopy, to detail atomic composition and effective work functions of these ITO surfaces. Electrochemical studies are also shown that indicate the fraction of the ITO surface which is electronically active and differences in electron transfer rates as a function of surface pretreatment. Studies of these chemisorbed probe molecules have led to a strategy for simple modification of the ITO surface using molecules which hydrogen bond or electrostatically adsorb to the ITO surface through their polar functional groups, but which present a non-polar face to enhance wettability by subsequently deposited organic layers. We also show first-generation experiments using non-optimized vacuum-deposited phthalocyanine/C₆₀-based PV cells, where the addition of simple organic modifiers improves both open-circuit photovoltages and short-circuit photocurrents relative to PV cells created on unmodified ITO surfaces.

2. Experimental

2.1. Cleaning/pretreatment of ITO substrates

The ITO/glass films used in these studies was obtained from Colorado Concept Coatings Limited, with a sheet resistance of ca. 13 Ω/cm². All ITO samples were initially cleaned by scrubbing with a soft cloth and a Triton X-100 solution, followed by ultrasonic cleaning in successive solutions of Triton X-100, water, and ethanol for at least 10 min each.

Four additional pretreatment/cleaning procedures were used in these studies which affected both the level of adventitious carbon and the coverage of hydroxide at the ITO surface [1]: (1) Air plasma cleaning (60 W for 5–15 min) was used for most devices. For all of the ITO films which were modified by small molecule

adsorbates and/or electropolymerized conducting polymer films, this air plasma cleaning step immediately preceded the modification and creation of the PV device; (2) Piranha treatment, a procedure adapted from Wilson and Schiffrin [28], consisted of three steps: (i) heating the ITO in a 10 mM solution of NaOH for 4 h at 80 °C, (ii) soaking the ITO in piranha (4:1 H₂SO₄: H₂O₂) for 1 min, and (iii) heating the ITO to ca. 160 °C for 2 h. The ITO film was then rinsed with copious amounts of water between each step. After this piranha treatment, we would characterize the resultant ITO surface by XPS/UPS and then return the thin film to a pH=10, EDTA solution, so as to dissolve any loosely held metal hydroxides (see text); (3) RCA treatment, a process which involved heating the ITO in a 1:1:5 solution of NH₄OH:H₂O₂:H₂O for 30 min at 80 °C, rinsing thoroughly with water, and drying with a stream of nitrogen gas; (4) Certain ITO samples were also argon-ion sputtered at 750 eV for 45 min with an argon pressure of 6.5×10⁻⁷ Torr, which were conditions estimated to remove some carbonaceous impurities and surface hydroxides, but which would not lead to extensive oxide reduction and lattice damage. The conditions for sputtering were such that the sputter-cleaned area was approximately 2 cm² and the sample was centered in this region to ensure that in subsequent electrochemical studies, the electrochemically active area was uniformly affected.

2.2. Surface modification of ITO thin films

Several different small molecules were adsorbed to the ultrasonically-cleaned, plasma etched ITO thin films, and then either used for the formation of PV films, or further modified with either spin-cast PEDOT:PSS (poly(3,4-diethoxy-thiophene):poly(styrene-sulfonate)), commercially available as Baytron-P-EL grade, Bayer Chemical Inc.), or with electrochemically grown PEDOT:ClO₄⁻ or PEDOT:PSS layers. In these studies two different small molecule adsorbates were evaluated: ferrocene dicarboxylic acid (Fc(COOH)₂) and 3-thiophene acetic acid (3-TAA) (both from Aldrich, used without further purification). Adsorption of Fc(COOH)₂ and 3-TAA onto ITO was achieved by soaking the ITO in a 1 mM solution of the small molecule, in pure ethanol, for 10–20 min and then rinsing briefly with acetonitrile [1,29].

Electrochemical characterization of the adsorbed monolayers was carried out by standard cyclic voltammetry. All electrochemistry was done with a saturated Ag/AgCl or a Ag wire reference electrode, a platinum counter electrode, and ITO as the working electrode. The potential axis of all voltammograms are reported vs. the ferrocene/ferricenium (Fc/Fc⁺) redox couple. The solvent for all the electrochemical studies of adsorbed small molecules was acetonitrile with a sup-

porting electrolyte of 0.1 M tetrabutylammonium hexafluorophosphate. PEDOT thin films were grown on the ITO substrate from solutions of 0.01 M 2,3-dihydrothieno[3,4-b]-1,4-dioxin (EDOT) and 0.1 M counter ion (LiClO_4), or 5 mg/ml PSS in acetonitrile. The potential was stepped to 1.1 V vs. Fc/Fc+ for periods of 1–5 s. After electropolymerization was stopped the potential was stepped back to +0.6 V, a value greater than that required to electrochemically dope PEDOT films but a value at which further PEDOT will not grow. The modified ITO substrate was then immersed under potential control, rinsed in ethanol, and dried in a stream of nitrogen.

2.3. Surface characterization of ITO thin films

XPS studies were conducted with a Kratos Axis-Ultra X-ray photoelectron spectrometer equipped with a monochromatic Al $K\alpha$ source at 1486.6 eV. For all the data presented here, the analyzed spot size was $300 \times 700 \mu\text{m}$, with an analyzer pass energy of 20 eV. UPS spectra were obtained with a pass energy of 5 eV and 21.2 eV He (I) excitation (Omicron VUV Lamp HIS 13). For all UPS analyses, a 5 V bias was applied to improve the transmission of low KE electrons and to improve the determination of the energy of the low KE edge [30]. The Fermi edge for these ITO samples was determined by extensive sputter cleaning of an ITO sample, until sufficient reduction of the surface was achieved to clearly see ionization from the Fermi edge of this material. We insured that the absolute kinetic energy of this edge was the same as seen for clean gold samples, i.e. the ITO samples were in electronic equilibrium with the spectrometer.

2.4. Formation and characterization of organic PV cells

The exact configuration of the PV cells is discussed further below. A phthalocyanine/ C_{60} multilayer configuration was selected which had been shown to provide power conversion efficiencies of ca. 2–3.6% [31], and which could be reproduced at lower, but consistent efficiencies in our labs. Multilayer cells were constructed in a vacuum chamber coupled to an Ar-glove-box/characterization chamber. We vacuum deposited sublimation-purified copper phthalocyanine (CuPc) (Aldrich), C_{60} (MER Corp.) and bathocuprine (BCP) (Aldrich); at ca. 1×10^{-6} Torr, on various cleaned and small molecule modified ITO substrates, over which we either spin cast PEDOT:PSS layers, or electrochemically grew PEDOT: ClO_4^- or PEDOT:PSS layers (see below). Following vacuum deposition of the final organic layer, we exposed these PV cells to atmosphere for ca. 5–10 min while a mask was fitted over the ITO substrate, the assembly was reintroduced to vacuum and an aluminum cathode (150 nm) was evaporated over the device. At

this point each ITO substrate had six PV devices adjacent to each other, which provided sufficient samples as to insure that the differences in performance between various surface modification steps were statistically significant. The PV cell was then immediately transported from the vacuum deposition environment into the glove box characterization environment—(final device structure = ITO/PEDOT:PSS (spin-cast; spin-cast over small molecule modifiers; electrochemically grown)/CuPc(20 nm)/ C_{60} (40 nm)/BCP(10 nm)/Al(150 nm)); device area = 2.6 mm^2 ; illumination = 250 W tungsten-halogen light source, diffused and IR filtered to provide ca. 25, 50, 75 or 100 mW/cm^2 incident white light.

3. Results and discussion

3.1. ITO surface composition and modification with probe molecules

Fig. 1a shows an AFM image of a typical commercial ITO thin film, following conventional solution cleaning procedures, and an air-plasma etch [1]. X-ray diffraction studies of such thin films have shown that the columnar structures seen in the AFM images of these sputter-deposited ITO films consist primarily of the $\langle 100 \rangle$ and $\langle 111 \rangle$ terminations of the In_2O_3 bixbyte lattice structure [32–35]. The rms roughness of commercially available ITO thin films can range from 1.5 to 3 nm, ‘amorphous’ ITO films, with reasonable electronic and electrochemical properties, can also be sputter-deposited with rms roughness values of ca. 0.5 nm. To achieve the desired optical and electrical properties required in OLED and PV applications, these films are intentionally produced with high concentrations of oxygen defects, and up to 10 mol% tin, substitutionally doped into the In_2O_3 bixbyte lattice, creating donor levels within ca. 0.03 eV of the conduction band ($\text{In}(5s)$) level [36,37]. The oxygen defect sites are especially susceptible to reaction with gas phase molecules, such as H_2O , carbonaceous materials, etc. during and just after the sputter deposition process, and it has been shown that In_2O_3 is naturally susceptible to hydrolysis (the hydrolysis constant is a factor of 10^{10} larger than for SnO_2) [38], leading to hydroxylated surfaces for the as-deposited thin films, and extensively hydrolyzed surfaces for ITO films that have been stored in atmosphere for lengthy periods [1–4,39].

O(1s) XPS peaks are the most useful photoemission data to characterize the different surface oxides formed on the ITO surface, and are summarized in Fig. 2a (upper left), at 75° take-off angles (to maximize surface sensitivity). These spectra are curve-fit and compared with standard oxides and hydroxides of indium and it can be clearly seen that these ITO surfaces are terminated in hydrolyzed oxides of indium and tin, including $\text{In}(\text{OH})_3$ and InOOH , which form immediately upon

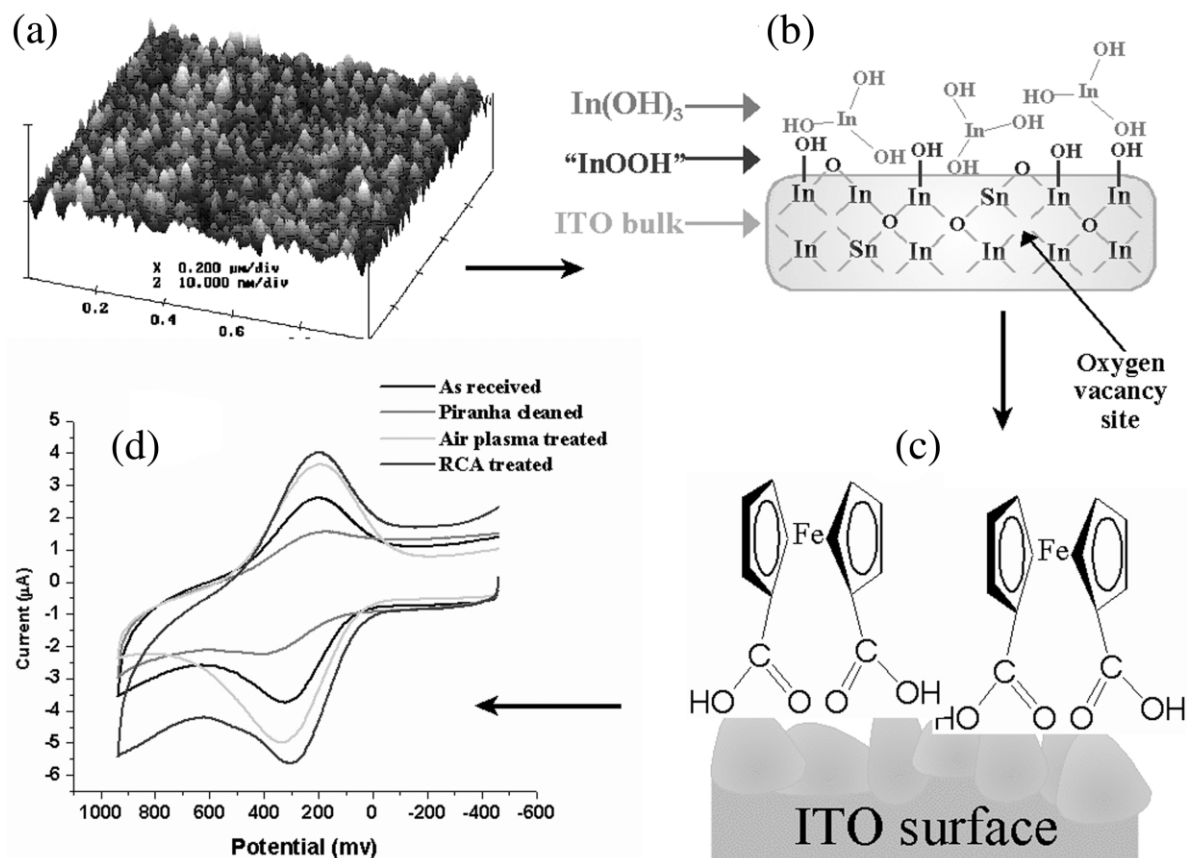


Fig. 1. (a) AFM image of a typical ITO sample, after cleaning but prior to chemical modification; (b) schematic view of the ITO surface showing the termination of the bixeyte lattice with both bridging and non-bridging oxygen atoms (the non-bridging sites are hydroxylated), and showing fully hydroxylated indium ($\text{In}(\text{OH})_3$) bound to the ITO surface; (c) schematic view of the chemisorption of $\text{Fc}(\text{COOH})_2$ to the ITO surface, placing the polar functional groups at the ITO interface, exposing the less polar ferrocene functionality; (d) cyclic voltammetry of chemisorbed $\text{Fc}(\text{COOH})_2$ monolayers on ITO surfaces pre-treated by various means. The largest $\text{Fc}(\text{COOH})_2$ coverages (highest peak currents) and highest rates of electron transfer are seen on the 'as-received' and air-plasma cleaned ITO. The smallest $\text{Fc}(\text{COOH})_2$ coverages and lowest electron transfer rates are seen on piranha cleaned ITO, even though this treatment produces the maximal number of hydroxylated surface sites. (Adapted from Ref. [1]).

exposure of the as-deposited ITO surface to atmosphere [1]. We have recently seen that these hydroxide surface groups can be mostly removed from the ITO surface by Ar-ion sputter-cleaning in the surface analysis environment, producing an O(1s) lineshape consistent with an In_2O_3 surface composition with only low levels of hydroxides [39]. Exposure of this sputter-cleaned surface to laboratory atmosphere for periods of only ca. 30 s, however, recreates the complex surface composition shown in Fig. 2a, i.e. hydrolysis of the ITO surface proceeds quickly after exposure of the oxide lattice to even laboratory atmospheric levels of H_2O .

The fraction of the surface existing in the stoichiometric oxide form, vs. hydroxides ($\text{In}(\text{OH})_x$) and oxyhydroxides (InOOH) can be controlled to some extent by cleaning/pre-treatment conditions. The highest concentration of hydroxide species arise from a procedure involving pretreatment of the ITO surface with piranha solution/concentrated NaOH (XPS data upper right in

Fig. 2a) [1,28]. In our hands this treatment produces one of the least electronically or electrochemically active ITO interfaces, but is useful as a way of determining the maximum extent of surface passivation and work function change which can result from formation of these hydroxides. Despite the high surface coverage of hydroxide species, which should be quite reactive toward silane coupling agents (e.g. hexamethy-disilazane, tetraphenyl-dimethyl-disilazane, and various tetraalkoxy or tetrachloro-silanes) [21,22,28], these piranha-treated surfaces show low coverages of the silane, suggesting that these molecules react predominantly with hydroxide surface species which are then easily removed (e.g. physically dislodged) from the ITO surface. A significant fraction of the hydroxide-like metal species can be removed through additional treatments of these ITO surfaces with the metal chelating agent, EDTA, (Fig. 2a, center), suggesting that the surface metal hydroxides produced by this treatment are disconnected from the

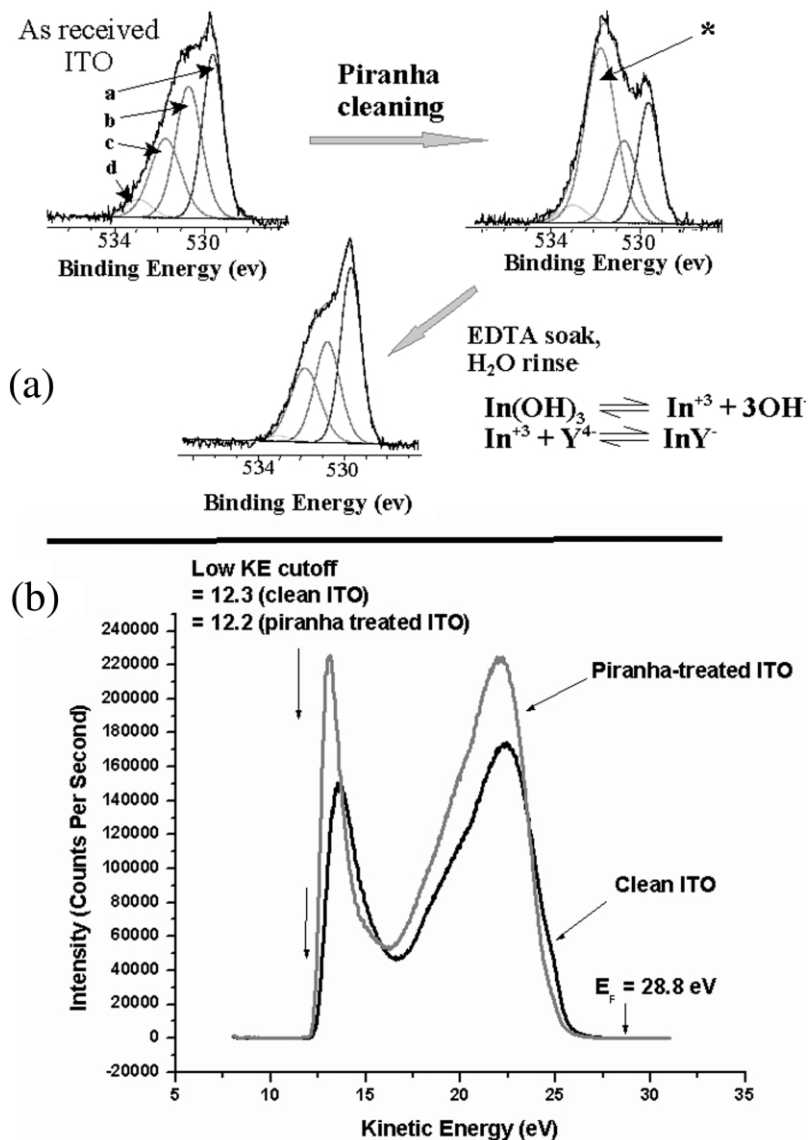


Fig. 2. (a) O(1s) XPS data (75° takeoff angle, to maximize surface sensitivity) for (upper left) 'as-received' ITO, (upper right) piranha-cleaned ITO, and (lower center) the piranha-cleaned ITO after treatment in an EDTA solution, followed by rinse and dry. These photoemission peaks can be divided into four oxygen components associated with (a) In_2O_3 ; (b) InOOH ; (c) In(OH)_3 and (d) and additional hydroxylated species (Ref. [1]). (b) He(I) UV-photoemission spectra of clean ITO (plasma etched, following normal cleaning), and of piranha-treated ITO. The difference in the source energy (21.2 eV) and the width of these photoemission spectra ($K_{E_{\text{ET,ITO}}}$ –low KE cutoff) give effective work functions of 4.7 and 4.6 eV for the plasma-etched and piranha-treated ITO films, respectively.

indium oxide lattice, and can be solubilized through complexation of the metal with the EDTA metal chelate [39,40]. The presumed chemical reactions which are relevant to this process include first of all the dissolution of In(OH)_3 to soluble products:



and the complexation of In^{+3} by EDTA(Y^{4-}) [40]:



The product of the solubility product for In(OH)_3 ($K_{\text{sp}} = 1.3 \times 10^{-37}$) and the formation constant for the In-EDTA complex ($K_f = 10^{25}$; pH=7), after correction for the real concentrations of EDTA used in this treatment (10^{-4} M), suggest that 'etching' of the ITO surface can occur, removing the equivalent of several monolayers of the most electrically inactive oxide/hydroxide materials [39].

Marks and coworkers have shown that it is possible to produce robust monolayer to multilayer films on ITO substrates using silane coupling chemistries, however, extensive cross-linking of the silane is required [21,22].

For such systems real enhancements in ITO stability can be expected, and the effective work function of the ITO substrate can be increased slightly. Improvements in OLED performance have been realized mainly by balancing the rates of hole and electron injection in such devices (decreasing hole injection rates to better match electron injection rates).

The effective work functions of these modified surfaces is determined by UV-photoelectron spectroscopy (UPS), using He(I) excitation sources [9–12,18,24,30,41]. This work function, Φ_{ITO} , is determined by the difference between the width of the photoemission spectrum (W =difference between the Fermi-edge energy, $E_{\text{F,ITO}}$, and lowest kinetic energy edge of the UPS spectral response), and the source energy: $\Phi_{\text{ITO}} = 21.2 \text{ eV} - W$. ITO thin films show widely varying work functions, depending upon source of ITO, surface cleaning procedures, modification with dipolar small molecule species, and addition of conducting polymer thin films, such as poly(3,4-diethoxy-thiophene)/poly(styrene)-sulfonates (PEDOT:PSS) [1–25]. Fig. 2b shows typical UPS spectra for a clean ITO sample, and for a piranha-treated ITO sample to determine the maximum work function difference produced by hydroxylation of the ITO surface. It is interesting to note that the effective work function of these two thin films is relatively unchanged by the presence of a large excess of metal hydroxides in the near surface region, a coverage of hydroxides which makes electron transfer reactions significantly slower than on the plasma-etched ITO samples (see below and Ref. [1]). Adsorption of the small molecules summarized below has to date produced only small work function changes in these ITO substrates, as revealed by UPS experiments, despite the fact that one predicts a small interface dipole effect from their chemisorption [41]. Larger changes have been noted for covalently bound modifiers, by Schwartz and coworkers [16–18], however, their modifiers are attached at surface sites which do not necessarily provide direct electrical contact to the oxide lattice. A more complete study of effective work function changes in ITO thin films as a function of pretreatment/chemical modification will be published elsewhere.

Chemisorption of small redox-active molecules to the ITO surface can be used to probe changes in electrochemical activity of the ITO surface as a function of surface pretreatment [1]. Several groups have noted that small molecules with carboxylic acid, or phosphonic acid functionalities will tightly chemisorb to the ITO surface, providing for changes in wettability, introduction of redox activity, and potentially the tuning of the effective surface work function [1,42–44]. Ferrocene dicarboxylic acid ($\text{Fc}(\text{COOH})_2$)—Fig. 1c), is chemisorbed from polar solvents, such as ethanol, to the pretreated ITO surface, and its electrochemical activity investigated by cyclic voltammetry in nonpolar solvents,

such as acetonitrile. We have assumed that a full, compact monolayer of $\text{Fc}(\text{COOH})_2$ adsorbs to each ITO surface, therefore, the peak currents for the oxidation/reduction of chemisorbed $\text{Fc}(\text{COOH})_2$ (Fig. 1d) are related to the coverage of electrochemically active material. The anodic–cathodic peak potential separation is used to determine electron transfer rates [1,45]. Both parameters vary significantly with ITO surface pretreatment conditions, from surface coverages of 2.2×10^{-11} – $1.8 \times 10^{-10} \text{ mol/cm}^2$ and apparent electron transfer rates from 0.17 s^{-1} to 0.8 s^{-1} [1]. The highest coverage of electroactive molecules and the highest electron transfer rates are obtained for ITO surfaces subjected to ultrasonic solution cleaning procedures (protocol described in Experimental section) followed by RF-plasma (air or O_2) etch, immediately preceding chemisorption of the probe molecule and immersion into the electrochemical cell. Coulometric analysis of these voltammograms, however, shows that we obtain only 40–50% of a compact monolayer coverage of electroactive $\text{Fc}(\text{COOH})_2$ on the most active ITO surface ($4 \times 10^{-10} \text{ mol/cm}^2$), even though chemisorption studies of $\text{Fc}(\text{COOH})_2$ on indium hydroxide surfaces shows that this chemisorption process proceed to a full monolayer coverage [1]. The implication is that half the available chemisorption sites on the ITO surface are typically disconnected from the conductive lattice. These results corroborate the recent results of Scherer and coworkers who showed by scanning tunneling microscopy that the typical ITO thin film surface consists of ‘patchy’ regions of quite variable conductivity with only approximately 50% of the ITO surface with high electrical conductivity [23].

3.2. ITO surface modification with molecules intended to optimize charge exchange and wettability

The variations in electroactivity of chemisorbed $\text{Fc}(\text{COOH})_2$ on ITO layers suggest that the physisorption of spin-cast conducting polymer layers (e.g. partially oxidized poly-anilines, PANI, or PEDOT:PSS), and other physisorbed surface modifiers on ITO, may make electrical contact with only a fraction of the electronically active ITO surface sites, which may ultimately become a limiting factor in the final optimization of OLED and PV technologies. This has been less of a problem of late in OLED technologies, where electron injection and transport are the emissive-state-limiting steps, and where lower rates of hole injection actually help balance the device, keeping the bulk of emissive state production away from the cathode. As better electron injection technologies are introduced, however, it will be desirable to enhance rates of hole injection. Hole and electron harvesting in organic PV technologies are both likely to require immediate optimization, and

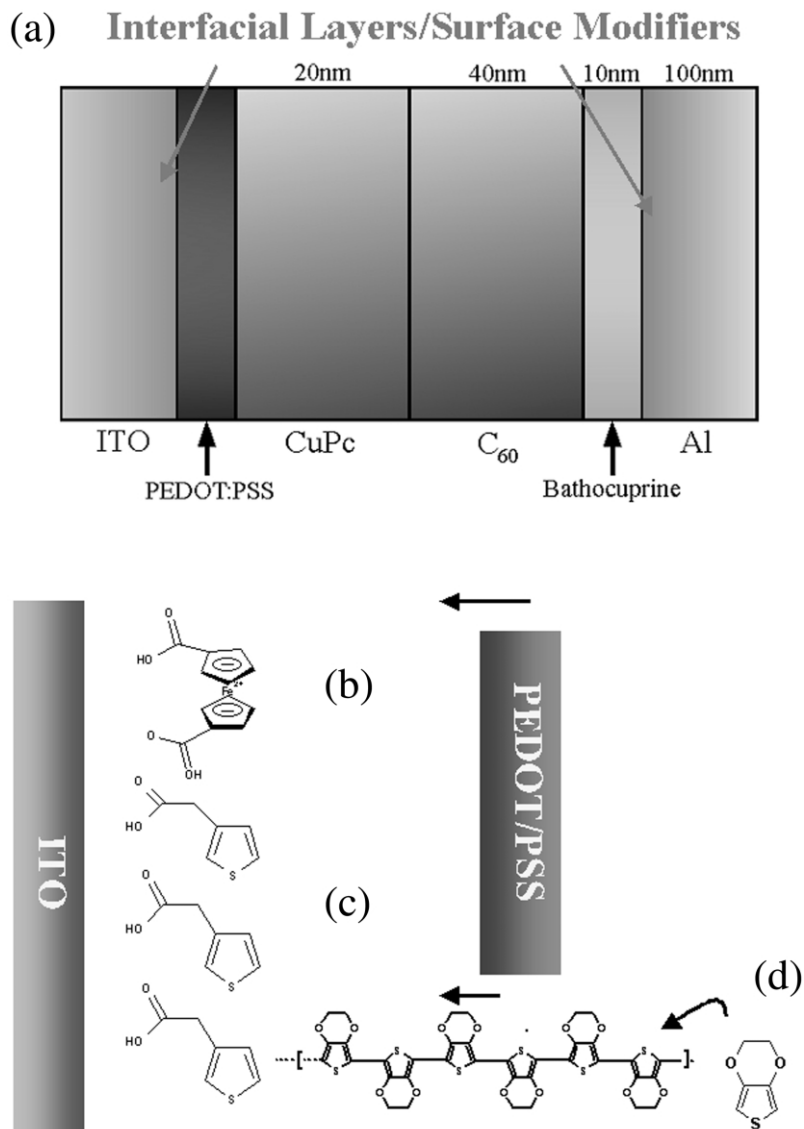


Fig. 3. (a) Schematic view of the vacuum-deposited PV cells used in this study, showing PEDOT:PSS layers on ITO that can be either spin cast on clean or small-molecule-modified, or that can be electrochemically grown (see text); CuPc(20 nm); C₆₀(40 nm); BCP(10 nm); followed by an Al cathode layer; (b) schematic views of small molecule surface modifiers, including (b) Fc(COOH)₂, (c) 3-TAA, and (d) electrochemically grown PEDOT over 3-TAA-modified ITO surfaces.

an appreciation that exciton dissociation may not be desirable at these interfaces.

Based on the extensive work done in the modification of electrochemically active oxide films, we have hypothesized that chemisorbed small molecules will provide for better direct electrical contact of added conducting polymer layers, and/or hole transport layers in OLED and PV technologies [43,44]. Fig. 3 shows schematic views of the chemisorption schemes which we are pursuing for the modification of ITO surfaces with Fc(COOH)₂, 3-thiophene acetic acid (3-TAA), and electrochemically-grown PEDOT over 3-TAA-modified ITO. The carboxy-substituted small molecules are believed to chemisorb with their polar head groups

toward the oxide surface providing a slightly more non-polar surface exposed to the next-deposited organic layers. Water contact angles for freshly cleaned, plasma-etched ITO surfaces are less than 10°. Contact angles for ITO surfaces immersed in EtOH (no small molecules) for 8 h, and then dried, increase to ca. 32°, whereas contact angles for ITO surfaces immersed in EtOH for 8 h, with millimolar concentrations of either Fc(COOH)₂ or 3-TAA, increase to 51° and 62°, respectively. These modifiers clearly increase the hydrophobicity of this polar oxide surface although not to the extent of covalently attached silane modifiers, where water contact angles in excess of 90° can be achieved [39,46]. It should be noted that none of these surface modifica-

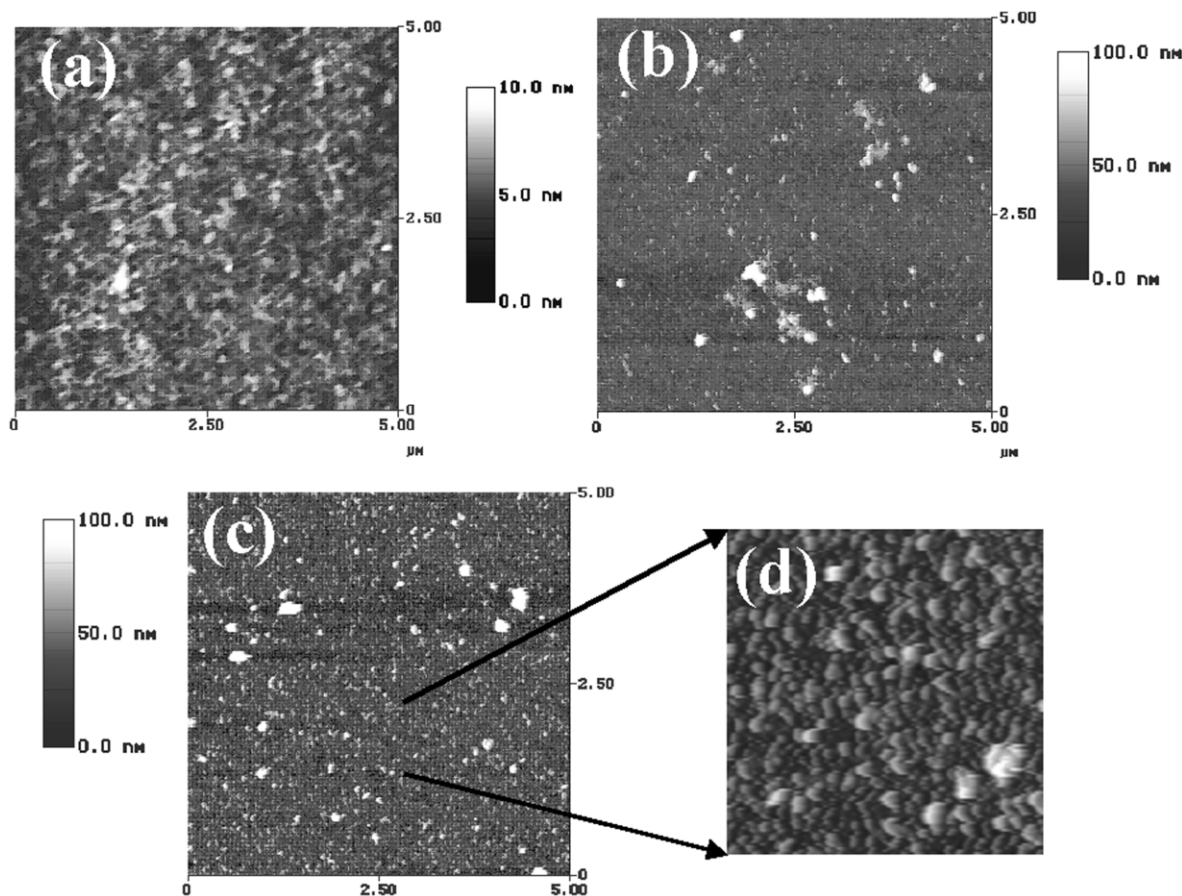


Fig. 4. 5×5 micron AFM images of (a) clean, plasma-etched ITO (z-scale 0–10 nm) and (b–c) PEDOT/ITO films, grown from acetonitrile solution (z-scale 0–100 nm) for 2.5 s and 5.0 s, respectively, (see text). The magnified view in (d) shows the ca. 0.1μ diameter dense nodular deposits of PEDOT on the surface in (c), arising from rapid nucleation of the electrochemically grown polymer.

tions, with chemisorbed small molecules, lead to noticeable changes in surface roughness, as explored with AFM, so that the changes in behavior described below do not seem to be attributable to changes in surface morphology of the ITO films themselves.

We have followed these chemisorption processes by either a) spin-casting of a PEDOT:PSS (Baytron-P-EL) layer, using conditions typical for most OLED and PV cells, or b) electropolymerization of the EDOT monomer, in the presence of either ClO_4^- counter ion, or a dilute solution of poly-(stryenesulfonate) to form either a doped PEDOT:PSS or PEDOT: ClO_4^- layer. Formation of PEDOT: ClO_4^- films on ITO (those discussed in this paper) was carried out in solutions of EDOT (0.01 M EDOT/acetonitrile/0.1 M LiClO_4), by stepping the ITO potential to ca. +1.1 V vs. Fc/Fc^+ for periods of time from 1–5 s, with and without prior modification of the ITO surface with 3-TAA. Our voltammetric experiments have shown that the onset potential for electropolymerization of EDOT decreases by ca. 0.1 V, and that at +1.1 V the current density for electropolymerization is at least a factor of 6x that seen for the clean ITO surface

[46]. This enhancement in kinetics of electropolymerization is consistent with the enhanced coverage of the EDOT monomer in the presence of the small molecule modifier, and the enhanced rate of formation of densely packed PEDOT nuclei on the ITO surface.

Fig. 4 shows AFM images of (a) the clean ITO surface, and (b–c) the same type of surface after PEDOT polymerization for 2.5 and 5 s at +1.1 V (3.9×10^{-8} mol/cm²; ca. 40 nm thickness) and 5.95×10^{-8} mol/cm²; ca. 60 nm thickness) respectively). Fig. 4d shows an enlargement of the AFM image in Fig. 4c, showing clearly the ca. 50–250 nm diameter PEDOT nuclei formed in the longer electrodeposition experiments. The rms surface roughness for this type of electrodeposited PEDOT is ca. 7 nm, over a $1 \times 1 \mu$ region, compared to an rms surface roughness of ca. 3 nm for spin-cast PEDOT:PSS films. Approximately 10% of the geometric surface area has somewhat larger PEDOT nuclei which have grown to heights and diameters nearly twice those of the surrounding regions, probably owing to preferred electrodeposition at the most electrically active ITO surface sites. Once these

PEDOT layers were formed, they were typically stepped back to +0.6 V vs. Fc/Fc⁺, a potential where electro-polymerization ceases but where the PEDOT film is still partially oxidized and conductive. These PEDOT:ClO₄⁻ modified ITO substrates were then immersed under potential control while rinsing in ethanol, dried and then immediately moved to the vacuum deposition chamber for completion of the multilayer PV cells.

3.3. Characterization of PV cells using modified ITO substrates

Characterization of these ITO substrates as anodes in PV cells was carried out with a vacuum-deposited multilayer configuration: (CuPc(20 nm)/C₆₀(40 nm)/BCP(10 nm)/Al(150 nm)), whose characteristics varied within acceptable limits from device-to-device, i.e. we could typically obtain the same current densities and photovoltages, within a few percent at each illumination flux, for all six devices on one ITO substrate, and little variation from day-to-day between groups of six PV devices. Peumans and Forrest have recently shown that this type of organic heterojunction PV cell can produce open circuit photovoltages (V_{OC}) of 0.35–0.5 V, short circuit photocurrents (J_{SC}) of 5–20 mA/cm², and power conversion efficiencies from 2–3.6% for white light illumination intensities ranging from 44 mW/cm² to 100 mW/cm², and that these values are strongly dependent upon surface pretreatment conditions for the ITO substrate [31]. In our laboratory this cell configuration was easily reproduced with day-to-day efficiencies of ca. 1% and allowed us to track changes in current/voltage behavior, cell efficiency, etc. as a function of changes in ITO modification procedure.

Thin film PV cells can be modeled as a simple photoactive diode, with an equivalent circuit as shown in the schematic in the inset of Fig. 5a. The current (J)/voltage (V) response of such cells has been modeled as [47,48]:

$$J = \frac{1}{1 + R_S/R_P} \times \left[J_0 \left\{ \exp\left(\frac{V - JR_S A}{nV_T}\right) - 1 \right\} - \left(J_{ph} - \frac{V}{R_P A} \right) \right] \quad (3)$$

and at zero-current the open circuit photovoltage, V_{OC} can be written as:

$$V_{OC} = nV_T \ln \left(1 + \frac{J_{ph}}{J_0} - \frac{V_{OC}}{J_0 R_P A} \right) \quad (4)$$

while the product of the short circuit photocurrent, J_{SC} and R_S can be written as:

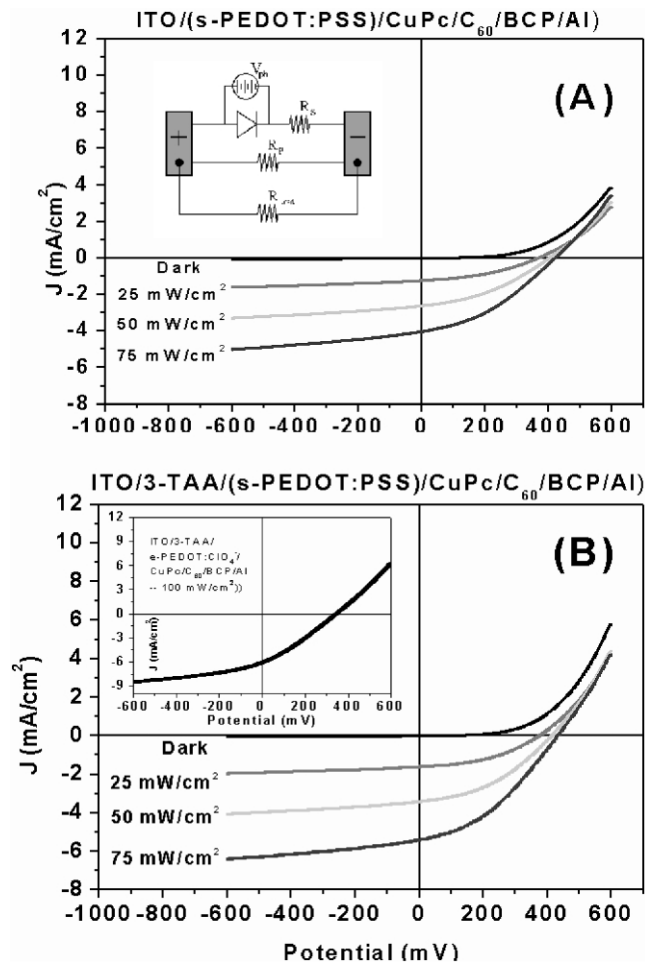


Fig. 5. (Inset upper right) Schematic view of the equivalent circuit for a typical PV cell, including the diode-like behavior, the shunt resistance, R_p , the series resistance R_s , and the external load resistance, R_L ; (central portion of figure) J/V plots for two ITO/CuPc/C₆₀/BCP/Al PV cells (ca. 50 mW/cm² white light illumination) with ITO substrates which are either (i) unmodified, (ii) modified with chemisorbed 3-TAA monolayers, prior to addition of a spin-cast PEDOT:PSS layer; (inset upper left) J/V response of a PV cell created from an ITO substrate modified with 3-TAA and an electrochemically grown PEDOT:ClO₄ layer (2.5 s, 1.1 V, see text) prior to deposition of the remainder of the PV assembly.

$$J_{SC} R_S = -\frac{nV_T}{A} \ln \left(1 + \frac{J_{ph}}{J_0} + \left(1 + \frac{R_S}{R_P} \right) \frac{J_{SC}}{J_0} \right) \quad (5)$$

where R_S is the series resistance and R_P is the shunt resistance (arising from pinholes and other short circuit pathways). Successful interface modifiers should maximize R_P by enhancing the wetting of the substrate to the deposited organic layers, through the formation of pin-hole free films. Lowering of V_{OC} values can arise from pin-holes, which short-circuit the PV cell, and through traps within the material and at the anode and cathode interfaces [47,48]. The major loss of PV power through lowered J_{SC} values originates from high values

of R_S . This series resistance is expected to arise from (i) the linear addition of contact resistances and the resistance to charge flow within the TCO film itself, (ii) resistances arising from low charge mobilities within the thin organic layers, and (iii) resistances arising from low rates of charge transfer at both the anode and cathode interfaces. The portion of R_S contributed by slow heterogeneous charge transfer, $R_{S,ET}$ is proportional to $1/k_{ET}$, where k_{ET} is the heterogeneous charge transfer rate coefficient (e.g. for oxidation/hole injection at the ITO/organic interface) [43,44]. The primary role of the ITO surface modifiers discussed here can, therefore, be to increase k_{ET} , by increasing the number of active sites for ET on the ITO surface, and possibly by lowering the reorganization energy for ET at the organic layer/ITO interface [43].

Fig. 5a and b are typical for PV data obtained for devices created on small molecule modified ITO, followed by spin-cast PEDOT:PSS layers, and on small molecule modified ITO surfaces on which the PEDOT layers were electrochemically grown. At white light intensities of 50 mW/cm^2 we compare PV cells with a chemisorbed monolayer of the small molecule modifier, e.g. 3-TAA, prior to addition of the PEDOT:PSS layer vs. PV cells made on unmodified ITO. V_{OC} increases by only a few millivolts (up to 0.414 V), J_{SC} increases significantly (from 2.6 to 3.4 mA/cm^2), only modest increases in fill factor are seen ($FF=0.38\text{--}0.40$), and the power conversion efficiency increases by ca. 40%, up to 1.14% for 3-TAA-modified ITO cells. Higher short circuit currents are observable for higher light intensities, with no loss of fill factor. Extrapolation of the J/V response under forward bias to the zero current axis allows estimation of series resistance, R_S , yielding values for the 3-TAA/s-PEDOT:PSS ITO surfaces as low as $3 \Omega \text{ cm}^2$. Comparable responses were obtained for ITO substrates modified with chemisorbed monolayers of $\text{Fc}(\text{COOH})_2$ (not shown).

Similar cells were constructed with electrochemically grown PEDOT films over the 3-TAA modifier, at both 2.5 and 5.0 s growth intervals. Results here are substantially more variable, indicating the need to further optimize the electropolymerization protocols, especially to control surface morphology of the electrochemically grown film, avoiding pinhole defects not encountered in the spin-cast PEDOT:PSS layers. The J/V response shown in the inset of Fig. 5b arises from a PV cell created on an ITO substrate with a PEDOT film grown for 2.5 s on a 3-TAA-modified ITO substrate, illuminated at 100 mW/cm^2 . J_{SC} values up to ca. 6.1 mA/cm^2 are achieved but with lower V_{OC} values (0.38 V) than the unmodified ITO films with spin-cast PEDOT:PSS layers. As seen with many other organic PV cells, [31] highest fill factors (ca. 0.5) are seen at the lowest illumination intensities (dropping to ca. 0.3 for the 100 mW/cm^2 illumination), and R_S values are decreased

from ca. $8 \Omega \text{ cm}^2$ to $4 \Omega \text{ cm}^2$ by the prior 3-TAA modification of the ITO substrate. Such decreases in R_S on PV cells which only differ by the simple modification of the ITO substrate and/or electrodeposition vs. spin-casting of PEDOT layers, confirms how critical the electrical contacts of these organic layers are to the ITO substrates in these emerging technologies.

We note that similar strategies have been recently adopted for the optimization of aluminum quinolate-based OLEDs, using small molecule modification of the ITO surface prior to addition of the PEDOT:PSS layer, and the vacuum deposition of the remainder of the OLED. The effect of the small molecule modifier in these devices is proving to be even more pronounced than shown here for vacuum deposited PV technologies, showing substantial reductions in leakage current, enhancements in space-charge-limited current densities, and significant enhancements in OLED efficiency. We attribute the bulk of these improvements to the fact that the PEDOT:PSS layers are more compatible with the modified ITO surface vs. the unmodified ITO surface, and that a greater fraction of the electrically active ITO surface is available to direct contact to the CP layer [46]. The results of these studies will be communicated shortly.

4. Conclusions

Transparent conducting oxide films are a critical component in energy conversion or display devices, and their importance is likely to only increase as these technologies evolve. Their surface chemistries, however, are complex and begin changing immediately upon first atmosphere exposure following their vacuum deposition. In the case of commercially available ITO thin films we and many other groups have noted the complexity of their surface composition, the variability in work function and electrical activity, and the difficulties in obtaining reproducible electrical performance from these materials. Modification of these anodes with spin-cast conducting polymer films, such as PEDOT:PSS, has been an appealing short-term solution to this problem, and has made possible many of the recent successes in optimization of OLED and PV technologies. As shown above it is unlikely that these spin-cast films take full advantage of the available electronically-active sites on the ITO surface, and that the current flow across the ITO/organic interface is still carried by only a fraction of the geometric area. Strategies designed to directly access the electronically active sites on the ITO surface, and to maximize the density of those sites, are clearly desirable.

We have shown here that simple chemisorbed small molecules can impact on the apparent series resistance in first-generation PV cells, using the assumption that a large fraction of that resistance arises from poor electri-

cal contact of the organic layers to the ITO surface, and low rates of heterogeneous electron transfer (hole injection or hole capture). Studies in progress seek to expand on this concept, and to provide additional modification strategies, which can be easily adapted to new PV and OLED technologies.

Acknowledgments

This research was supported in part by grants from the Office of Naval Research, the Department of Energy/National Renewable Energy Laboratories, and the National Science Foundation (Chemistry). C. Donley gratefully acknowledges receipt of support through a Pfizer graduate fellowship, and a Division of Analytical Chemistry/ACS graduate fellowship.

References

- [1] C. Donley, D. Dunphy, D. Paine, C. Carter, K. Nebesny, P. Lee, D. Alloway, N.R. Armstrong, *Langmuir* 18 (2002) 450.
- [2] J.S. Kim, M. Granstrom, R.H. Friend, N. Johansson, W.R. Salaneck, R. Daik, W.J. Feast, F. Cacialli, *J. of Appl. Phys.* 84 (1998) 6859.
- [3] J.S. Kim, B. Lagel, E. Moons, N. Johansson, I.D. Baikie, W.R. Salaneck, R.H. Friend, F. Cacialli, *Synth. Met.* 111 (2000) 311.
- [4] J.S. Kim, R.H. Friend, F. Cacialli, *J. Appl. Phys.* 86 (1999) 2774.
- [5] C. Ganzorig, M. Fujihira, *Appl. Phys. Lett.* 77 (2000) 4211.
- [6] C. Ganzorig, K.J. Kwak, K. Yagi, M. Fujihira, *Appl. Phys. Lett.* 79 (2001) 272.
- [7] X. Zhou, M. Pfeiffer, J. Blochwitz, A. Werner, A. Nollau, T. Fritz, K. Leo, *Appl. Phys. Lett.* 78 (2001) 410.
- [8] T. Kugler, W.R. Salaneck, H. Rost, A.B. Holmes, *Chem. Phys. Lett.* 310 (1999) 391.
- [9] G. Greczynski, T. Kugler, M. Keil, W. Osikowicz, M. Fahlman, W.R. Salaneck, *J. Electron Spectrosc. Relat. Phenom.* 121 (2001) 1.
- [10] J.S. Kim, B. Lagel, E. Moons, N. Johansson, I.D. Baikie, W.R. Salaneck, R.H. Friend, F. Cacialli, *Synth. Met.* 111 (2000) 311.
- [11] Q.T. Le, F. Nuesch, L.J. Rothberg, E.W. Forsythe, Y.L. Gao, *Appl. Phys. Lett.* 75 (1999) 1357.
- [12] Q.T. Le, F.M. Avendano, E.W. Forsythe, L. Yan, Y.L. Gao, C.W. Tang, *J. Vac. Sci. Technol. a-Vac. Surf. Films* 17 (1999) 2314.
- [13] R.A. Hatton, M.R. Willis, M.A. Chesters, F.J.M. Rutten, D. Briggs, *J. Mater. Chem.* 13 (2003) 38.
- [14] V. Christou, M. Etchells, O. Renault, P.J. Dobson, O.V. Salata, G. Beamson, R.G. Egdell, *J. Appl. Phys.* 88 (2000) 5180.
- [15] E.W. Forsythe, M.A. Abkowitz, Y.L. Gao, *J. Phys. Chem. B* 104 (2000) 3948.
- [16] D.J. Milliron, I.G. Hill, C. Shen, A. Kahn, J. Schwartz, *J. Appl. Phys.* 87 (2000) 572.
- [17] K.L. Purvis, G. Lu, J. Schwartz, S.L. Bernasek, *J. Amer. Chem. Soc.* 122 (2000) 1808.
- [18] E.L. Bruner, N. Koch, A.R. Span, S.L. Bernasek, A. Kahn, J. Schwartz, *J. Amer. Chem. Soc.* 124 (2002) 3192.
- [19] K. Sugiyama, H. Ishii, Y. Ouchi, K. Seki, *J. Appl. Phys.* 87 (2000) 295.
- [20] J.A. Chaney, P.E. Pehrsson, *Appl. Surf. Sci.* 180 (2001) 214.
- [21] J. Cui, A. Wang, N.L. Edleman, J. Ni, P. Lee, N.R. Armstrong, T.J. Marks, *Adv. Mater.* 13 (2001) 1476.
- [22] J.E. Malinsky, J.G.C. Veinot, G.E. Jabbour, S.E. Shaheen, J.D. Anderson, P. Lee, A.G. Richter, A.L. Burin, M.A. Ratner, T.J. Marks, N.R. Armstrong, B. Kippelen, P. Dutta, N. Peyghambarian, *Chem. Mater.* 14 (2002) 3054.
- [23] Y.H. Liao, N.F. Scherer, K. Rhodes, *J. Phys. Chem. B* 105 (2001) 3282.
- [24] R. Schlaf, H. Murata, Z.H. Kafafi, *J. Electron. Spectrosc. Relat. Phenom.* 120 (2001) 149.
- [25] H.Y. Yu, X.D. Feng, D. Grozea, Z.H. Lu, R.N.S. Sodhi, A.M. Hor, H. Aziz, *Appl. Phys. Lett.* 78 (2001) 2595.
- [26] (a) D.R. Dunphy, S.B. Mendes, S.S. Saavedra, N.R. Armstrong, *Anal. Chem.* 69 (1997) 3086
(b) J.T. Bradshaw, S.B. Mendes, N.R. Armstrong, S.S. Saavedra, *Anal. Chem.* 75 (2003) 1080.
- [27] (a) P.M. Armisted, H.H. Thorp, *Anal. Chem.* 72 (2000) 3764
(b) N.D. Popovich, S.S. Wang, B.K.H. Yen, H.Y. Yeom, D. Paine, *Anal. Chem.* 74 (2002) 3127.
- [28] R. Wilson, D.J. Schiffrin, *Analyst* 120 (1995) 175.
- [29] G. Zotti, G. Schiavon, S. Zecchin, A. Berlin, G. Pagani, G. Langmuir 14 (1998) 1728.
- [30] R. Schlaf, B.A. Parkinson, P.A. Lee, K.W. Nebesny, N.R. Armstrong, *J. Phys. Chem. B* 103 (1999) 2984.
- [31] P. Peumans, S.R. Forrest, *Appl. Phys. Lett.* 79 (2001) 126.
- [32] H.Y. Yeom, N. Popovich, E. Chason, D. Paine, *Thin Solid Films* 411 (2002) 17.
- [33] N. Popovich, S.S. Wong, B.K. Yen, H. Yeom, D.C. Paine, *Anal. Chem.* 74 (2002) 3127.
- [34] D.C. Paine, T. Whitson, D. Janiac, R. Beresford, C.O. Yang, B. Lewis, *J. Appl. Phys.* 85 (1999) 8445.
- [35] C.W. Ow-Yang, D. Spinner, Y. Shigesato, D.C. Paine, *J. Appl. Phys.* 83 (1998) 145.
- [36] J.C.C. Fan, J.B. Goodenough, *J. Appl. Phys.* 48 (1977) 3524.
- [37] H.L. Hartnagel, A.L. Dawar, A.K. Jain, C. Jagadish, *Semiconducting Transparent Thin Films*, Institute of Physics Publishing, Bristol, 1995, p. 13–15, 175–187, 265–282.
- [38] C.F. Baes Jr, R.E. Mesmer, *The Hydrolysis of Cations*, John Wiley and Sons, New York, 1976, p. 319–327, 349–357.
- [39] C. Donley, C. Carter, unpublished results.
- [40] D.C. Harris, *Quantitative Chemical Analysis*, 5th ed, WH. Freeman and Co, New York, 1999, p. 313, and AP 12–14.
- [41] (a) H. Ishii, K. Sugiyama, E. Ito, K. Seki, *Adv. Mat.* 11 (1999) 605
(b) D. Cahen, A. Kahn, *Adv. Mater.* 15 (2003) 271.
- [42] T.J. Gardner, C.D. Frisbie, M.S. Wrighton, *Am. J. Chem. Soc.* 117 (1995) 6927.
- [43] I. Rubenstein, in: I. Rubenstein (Ed.), *Physical Electrochemistry*, Marcel Dekker, Inc, New York, 1995, pp. 13–17, and references therein.
- [44] R.W. Murray, *Molecular design of electrode surfaces*, in: R.W. Murray (Ed.), *Techniques of Chemistry Series*, 22, John Wiley and Sons Inc, New York, 1992, pp. 1–48, and references therein.
- [45] E. Laviron, *J. Electroanal. Chem.* 101 (1979) 19.
- [46] C. Carter, A. Simmonds, unpublished results.
- [47] S. Fonash, *Solar Cell Device Physics*, Academic Press, New York, 1981, pp. 133–184.
- [48] B.A. Gregg, M.C. Hanna, *J. Appl. Phys.* 93 (2003) 3605.